sciendo

CIVIL AND ENVIRONMENTAL ENGINEERING REPORTS

E-ISSN 2450-8594

CEER 2022; 32 (2): 0154-0173
DOI: 10.2478/ceer-2022-0024
*Original Research Article*

# NUMERICAL INVESTIGATION OF SQUARE FOOTING POSITIONED ON GEOCELL REINFORCED SAND BY USING ABAQUS SOFTWARE

Gaurav JUNEJA[1], Ravi Kumar SHARMA[2]
[1]Research Scholar, Civil Engineering Department, NIT Hamirpur (HP), India
[2]Professor, Civil Engineering Department, NIT Hamirpur (HP), India

A b s t r a c t

The usage of geocell reinforcement for foundations supported on weak soil has been increased these days. The purposed study uses FEM-based ABAQUS software to analyse the behaviour of square footing supported on geocell reinforced sands subjected to static vertical loading. Numerical analysis was performed to find the optimum combination of the different geometric parameters of the geocell reinforcement. Three distinct types of sands were employed in the study with relative densities of 30%, 50%, and 70%. The geometric parameters of the geocell, such as the placement depth of geocell (u), the width (b), and the height (h) of the geocell, were modified in relation to the footing width (B) to access the optimum combination ratios. The inclusion of the geocell reinforcement increases the load-carrying capacity up to 5-6 times compared to unreinforced sand. The results obtained from the numerical analysis were intended to correlate well with the experimental data available in the literature.

Keywords: square footing, geocell reinforcement, sand, FEM

[1] Corresponding author: Research Scholar, Civil Engineering Department, NIT Hamirpur (HP), India, e-mail: juneja.gaurav@nith.ac.in

## 1. INTRODUCTION

The need for structures built on poor/weak soil has increased as a result of the fast development of infrastructures and urbanization. There are various techniques developed by geotechnical engineers to enhance the behaviour of weak soil in terms of strength, stiffness of soil and reduce the vulnerability to liquefaction [1-3]. Among the various ground improvement techniques available, such as replacing poor soil with good-fill soil, using various chemical treatments, cement grouting, preloading with vertical drains, and so on, soil reinforcement in various modified forms is widely admired for its cost, technical, and environmental versatility [4-5]. From the various soil reinforcement techniques, geosynthetics are regarded as a long term and cost-effective option. The use of geosynthetics in building construction and pavement has yielded several benefits such as reduced settlements, increased bearing capacity, and so on. Many geotechnical engineers employ Geocell, a modified version of geosynthetics, as a soil reinforcing material. Geocell is a three-dimensional honeycomb-like structure that confines the infill material in three dimensions. The lateral outspreading of the infill material is limited due to the all-around confinement offered by the geocell. The beneficial results of the geocell reinforcement were reported by many researchers by using field studies and experimental studies [6-12]. Although, for the design of complex geotechnical problems only experimental and field studies are not sufficient. Because these studies are time-consuming. For the design of geocell reinforcement, quick results are required to analyse the effect of various parameters. In that case, the numerical modelling technique is the best choice. Numerical modelling of the geocell is very difficult due to its complicated honeycomb structure. Many researchers employ the equivalent composite technique to analyse geocell reinforced soil models. Soil and geocell are considered composite materials with increased stiffness and strength in this method [13-15]. This technique to geocell modelling is unrealistic, and it also avoids the unpredictability associated with parametric variation. Geocell is a three-dimensional honeycomb structure, a three-dimensional modelling approach should be used to model the geocell. The three dimensional analysis of geocell reinforced sand foundation system for different geometric combinations of the geocell has been studied by various researchers [9, 16-21]. The analysis of geocell reinforced sub-ballast has been done by using Federal Highway Administration (FHWA) and Drucker-Prager yield criteria [22-23]. The actual honeycomb shape of the geocell rather than square and circular geometry has been modelled by using FEM software to analyse the behaviour of the geocell reinforcement [24-25]. The effectiveness of the geocell reinforced for shell foundation has been investigated by using PLAXIS 3D [26]. Some researchers have given analytical solution to evaluate the settlement and stress propagation in the geocell reinforced soil [27-

28]. As a result of the studies mentioned above, it can be concluded that geocell reinforcement are better and cost-effective to increase the bearing capacity of the poor soil. Most of the experimental and analytical studies available in literature uses the square, circular and curved honeycomb shape of the geocell reinforcement. Limited studies are available, using the hexagonal geometry of the geocell reinforcement subjected to static vertical loading. Hexagonal geometry possesses highest surface/perimeter ratios. Hence, the hexagonal shape of the geocell requires the least amount of material to hold the maximum weight and all the six sides of the geocell fixed perfectly together compared to other polygon shapes. The hexagonal structure of the geocell distribute the stress uniformly along the perimeter of the geocell. Hence, an attempt has been made in the present study to analyse the effect of relative density of the sand below the foundation on the performance of geocell reinforcement having hexagonal geometry subjected to static vertical loading using ABAQUS software.

## 2. FINITE ELEMENT MODELLING AND SOIL PROPERTIES

The finite element approach was used in this work to analyse the behaviour of a concentrated loaded footing placed on geocell reinforced sand using ABAQUS software. Square shaped footing of size (B) 75mm resting on geocell reinforced sand having different properties was used for numerical modelling as shown in Figure 1. The lateral and base mobility of the soil was inhibited in all three directions. For the analysis, the plan dimension of the sand was taken as 500mm × 500mm for length and breadth and 350mm for depth. To neglect the boundary effects, the distance between the soil model boundary and the foundation edges was set at 6.5B in the x and y directions and 4.5B in the z-direction [29]. The three-dimensional honeycomb structure of geocell having hexagonal geometry has been modelled by using ABAQUS software. The properties of the geocell employed in the numerical study were chosen as per [30], summarised in Table 1. The aperture size of the geocell cell was taken as 0.8B, geocell placement depth (s) from the footing base was varied from 0B to 0.4B, width (b) was varied from 1B to 5B, and height (h) was varied from 0.5B to 2B.

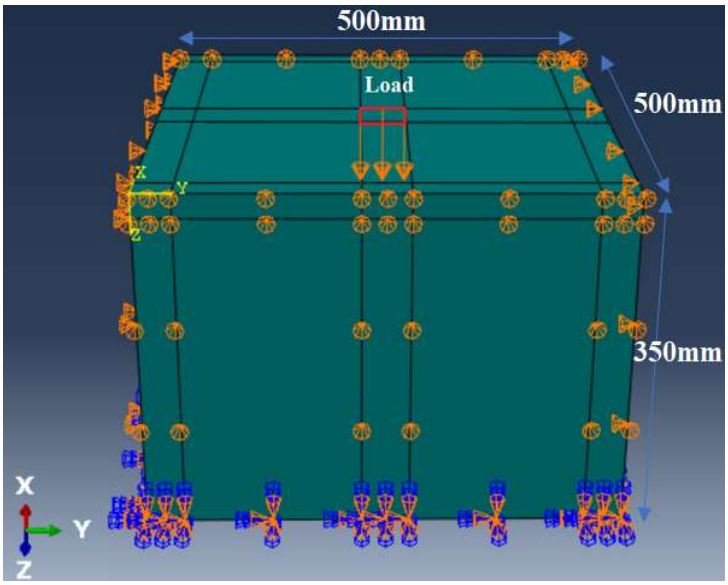


(a)

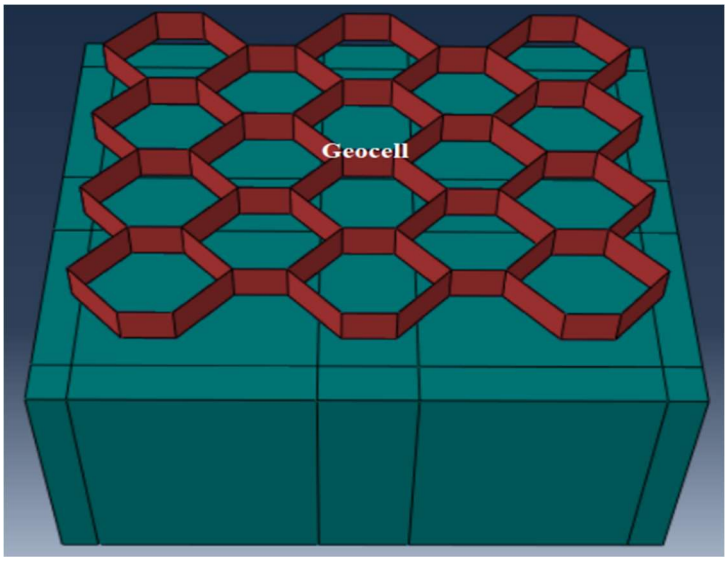


(b)

Fig. 1. Numerical models of geocell reinforced sand subjected to vertical loading (a) loading diagram and boundary conditions (b) geometry of geocell embedded in sand

Table 1. Geocell properties used for numerical modelling

| Cell size, mm | Geocell wall thickness, mm | Unit weight (γ), Kg/m$^3$ | Poisson's ratio (μ) | Young's modulus (E), MPa |
|---|---|---|---|---|
| 60.5×62 | 1.5 | 950 | 0.3 | 275 |

Table 2 summarised the usage of three distinct sands with various properties in the current investigation. The friction angles (Ø) of the sands corresponding to the varied relative densities ($R_d$) of 30%, 50%, and 70% were taken to be 36.06˚, 39.08˚, and 42.05˚, respectively. The magnitude of the dilation angle (Ψ) was computed by the relation Ψ = Ø-30 given by [31] and the Modulus of elasticity (E) of the sand was determined as per the range given by [32]. From the range recommended by [33], Poisson's ratio (υ) of sand was taken as 0.3. The soil-geocell interface was assumed to be partially rough, with an interface friction factor (δ) of magnitude 0.8 corresponds to the similar value taken by [26]. The detailed numerical analysis test layout of the different properties of sand and different geometric combinations of the geocell used are presented in Table 3.

Table 2. Sand properties used for numerical modelling

| Relative density ($R_d$) | Friction angle (Ø) | Dilation angle (Ψ) | Cohesion (C), kPa | Unit weight (γ), Kg/m$^3$ | Poisson's ratio (μ) | Young's modulus (E), MPa |
|---|---|---|---|---|---|---|
| 30% | 36.06˚ | 6.06˚ | 0.1 | 1415 | 0.3 | 18 |
| 50% | 39.08˚ | 9.08˚ | 0.1 | 1620 | 0.3 | 50 |
| 70% | 42.05˚ | 12.05˚ | 0.1 | 1910 | 0.3 | 60 |

## 3. FINITE ELEMENT MESH

In the present study, the modelling of sand has been done using Mohr-Coulomb criteria. Mohr-Coulomb criteria require less property input parameters and less computation time for the analysis compared to Drucker-Prager yield criteria [29]. The geocell geometry was modelled using the shell element. The general meshing obtained for numerical analysis is shown in Figure 2. A very fine mesh takes more computation time for the analysis whereas a very coarse mesh is not able to express the important behaviour of the particular domain. Hence, finer to coarser mesh was used for the numerical modelling. Finer mesh is used near the square footing and coarser mesh is used as the distance increased from the footing. Because of the intricate honeycomb structure of the geocell, the geocell model employed with global mesh. An 8-node linear brick (C3D8R) element was used for modelling. According to the convergence analysis, the optimal number of elements produced in this analysis for soil model 6877 and for geocell was 687.

Further increasing the number of elements, marginal increment is observed in the bearing capacity.

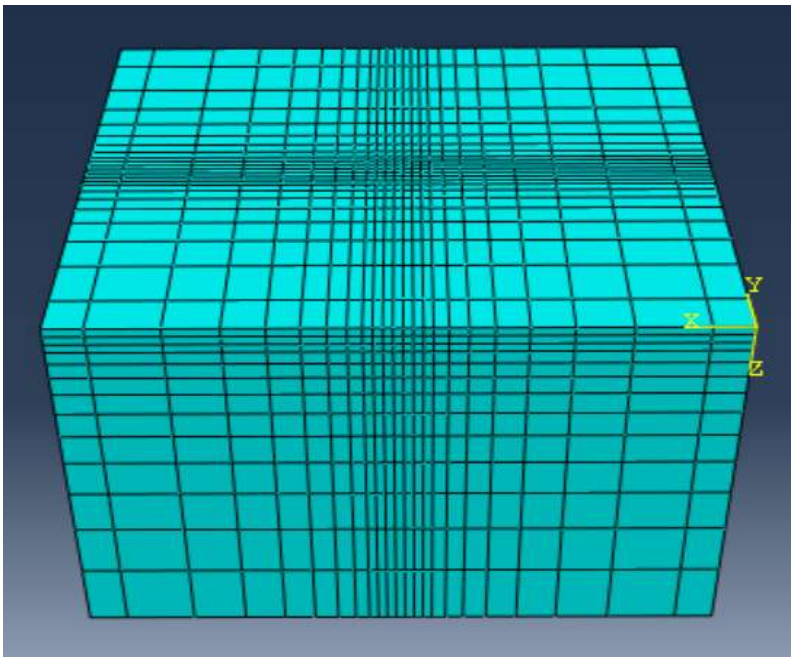


Fig. 2. Meshing of square footing with geocell reinforced sand

## 4. RESULTS AND DISCUSSION

The numerical analysis of geocell reinforced sand subjected to concentrated loaded square footing yielded the following results. For the analysis, various geocell geometric parameters such as placement depth (u), geocell layer width (b), and geocell height (h) are used. The bearing capacity improvement factor ($I_f$) is used to express the improvement in the behaviour of a geocell reinforced foundation system. It is expressed as the ratio of bearing capacity of reinforced sand to the bearing capacity of unreinforced sand [8,12]. The specified displacement (s) is expressed as s/B (%) of the footing width. The improvement factor ($I_f$) for different numerical modelling tests (S No. 2 – S No. 4) are presented in Table 4.

Table 3. Numerical Modelling test details

| S. No. | Details | Variable parameters | Constant parameters |
|---|---|---|---|
| 1. | Unreinforced sand | $R_d$ = 30%, 50%, 70% | |
| 2. | Effect of placement depth of geocell below footing base | u/B = 0, 0.1, 0.2, 0.3, 0.4 | $R_d$ = 30%, h/B =1.5, b/B = 5 |
| 3. | Effect of width of the geocell layer | b/B = 1, 2, 3, 4, 5 | $R_d$ = 30%, h/B =1.5, u/B = 0.1 |
| 4. | Effect of height of the geocell | h/B = 0.5, 1, 1.5, 2 $R_d$ = 30%, 50%, 70% | u/B = 0.1, b/B = 5 |

## 4.1. Effect of geocell placement depth below footing base

The numerical analysis was performed for different placement depth of the geocell layer (u) below the footing base. Figure 3 depicts the pressure settlement results for varying depths of the geocell layer below the footing base. From the results obtained, it was observed that the load carrying capacity of the geocell reinforced sand was improved by increasing the placement depth from 0B to 0.1B and further increasing the depth from 0.1B to 0.4B there is decrease in the effectiveness of the geocell layer. When the geocell layer are placed at immediate contact with the footing base (u/B =0), buckling of the walls of the geocell may takes place during the application of load [7]. Hence, the effectiveness of the geocell reinforcement may get reduced. The percentage increase in bearing capacity was found to be 31.77% with increasing the placement depth from 0B to 0.1B. With the presence of sand layer between the footing base and geocell avoids the immediate contact between them and prevents the buckling of the geocell walls during load application, hence the effectiveness of the geocell gets increased compared to geocell placed immediate contact with the footing base. With increasing the placement depth of the geocell beyond 0.1B, there is decrease in the load carrying capacity is observed. This is due to because with the increase in thickness of sand cushion between the footing base and geocell, lateral spreading of sand mass takes place during load application. Figure 4 presents the result drawn between improvement factor ($I_f$) and different placement depth of the geocell layer (u/B) at different settlements 2%, 5%, 10% and 15% of the footing size. At 15% settlement, the improvement factor was improved from 4.13 to 6 for the placement depth of the geocell varied from 0B to 0.1B. Further increase in the depth of the geocell to 0.2B, 0.3B and 0.4B the improvement factor was decrease to 5.2, 4.98

and 4.78. As a consequence, the findings clearly show that the optimum geocell placement depth is at u = 0.1B below the footing base.

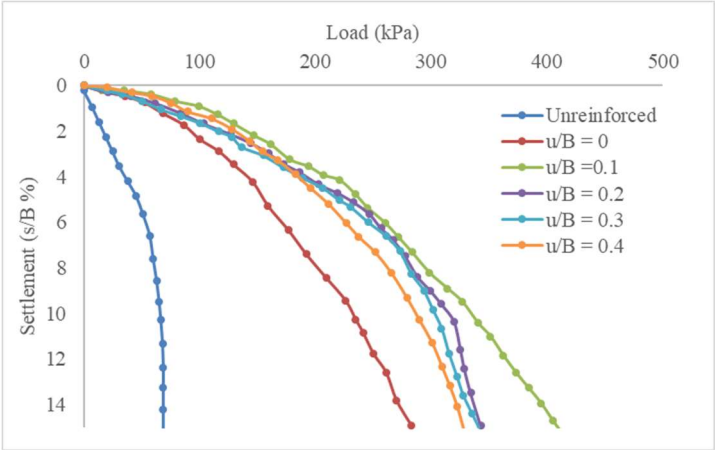


Fig. 3. Load-settlement ratio for different placement depth of the geocell below the footing base

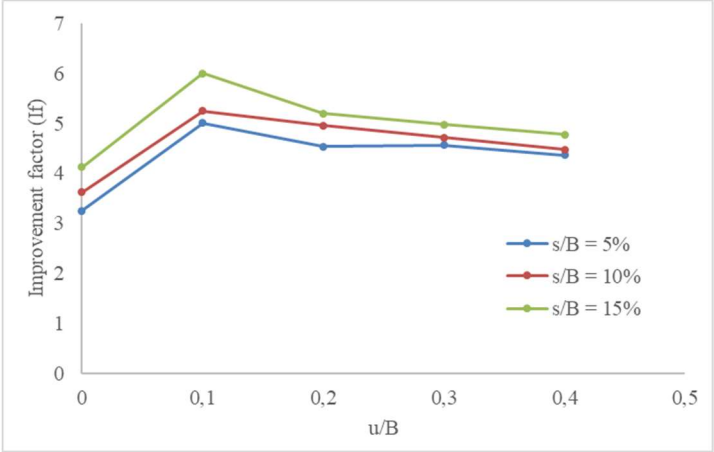


Fig. 4. Variation of improvement factor ($I_f$) for different placement depth (u) of the geocell at different s/B% ratios

## 4.2. Effect of geocell width

The numerical analysis was carried out on geocell reinforced foundation system placed on sand for different width ratio (b/B) of the geocell mattress. Figure 5 presents the results for load-settlement behaviour of geocell reinforced sand for different width of the geocell layer. Figure 6 presents the result drawn between improvement factor ($I_f$) and different width (b) of the geocell layer for different

settlement ratios. From the obtained results, it can be perceived that with increasing the width of the geocell layer there is increase in the load carrying capacity of the geocell reinforced sand for all prescribed displacements. This is due to because, with increasing the width of the geocell there is an increase in the confining area for sand by increasing the number of interconnected cells. Hence, results in increasing rigidity of the soil and offered greater shear resistance for the lateral mobilization of the sand during the application of load. The percentage gain in the load carrying capacity was found to be 38.84% when the width of the geocell (b) was increased from 1B to 2B. Further increasing the geocell width beyond 2B to 3B and 3B to 4B the percentage improvement was found to be 9.72% and 9.84%. Alternatively, increasing geocell layer width from 4B to 5B very marginal improvement 3.51% was observed. The effectiveness of the geocell reinforcement beneath the footing base is limited to a certain width, after which it improves marginally. [4] reported that the optimum width of the geocell is 4.9B, beyond this width the improvement was found to be very marginal. Reference [12] reported the optimum width of the geocell was 4B in his study for jute geocell. The alteration in the optimum width of the geocell reinforcement in different studies was attributable to variables such as varied soil parameters and different geocell reinforcement properties used.

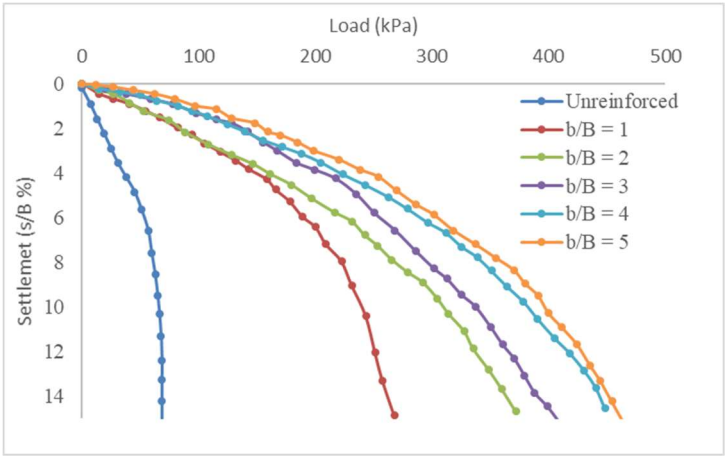


Fig. 5. Load-settlement ratios for different width of the geocell

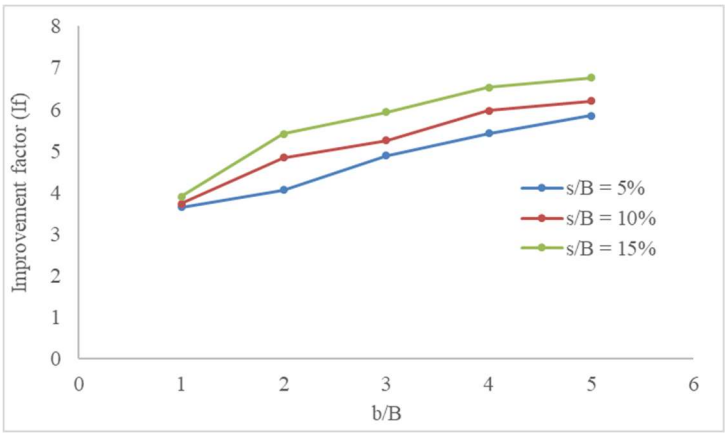


Fig. 6. Variation of improvement factor ($I_f$) for different width (b) of the geocell at different s/B% ratios

## 4.3. Effect of geocell height

The numerical analysis was performed to investigate the effect of varying height ratios (h/B) of the geocell mattress. Figure 7 present the load-settlement plots for varying height (h) of the geocell mattress at different relative densities (30%, 50% and 70%). The obtained findings revealed that geocell reinforcement is effective up to a specific height of the geocell mattress; however, as the height of the geocell increases, the improvements become extremely minimal. The results indicate that maximum improvement in load carrying capacity is obtained at 1.5B height of the geocell, and beyond this increasing the height from 1.5B to 2B results in very marginal improvement in load carrying capacity. With increasing the height of the geocell mattress, confined area for the soil gets increased. The soil confinement tends to increases the rigidity of the geocell layer and allowing the footing load to be distributed over a larger area. Furthermore, as the height of the geocell mattress increases, the adhesive resistance provided for sand particle mobilisation in the lateral direction increases during load application. The improvement in load carrying capacity is found to be marginal beyond h/B ratio of 1.5 due to lateral buckling of the geocell walls on load application. Figure 8 depicts the plots of the improvement factor versus varying height ratios (h/B) at various settlements. Reference [6] reported that increasing the height of the geocell mattress beyond h/B ratio 2.1 causes lateral buckling of the geocell walls, results in reducing the performance of the geocell reinforcement.

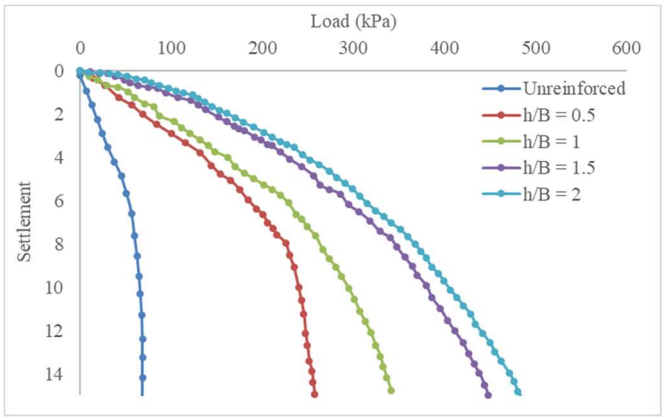


(a)

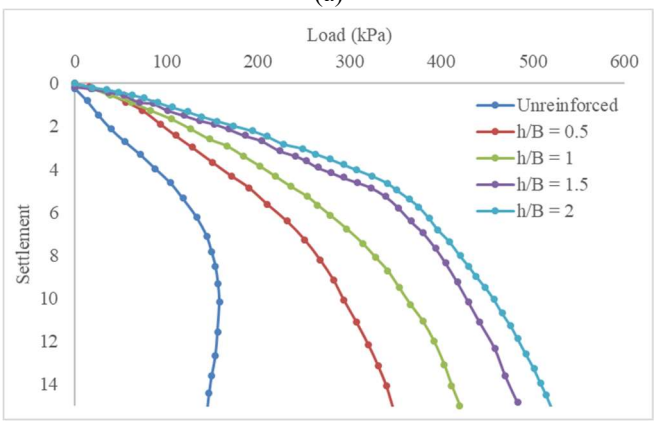


(b)

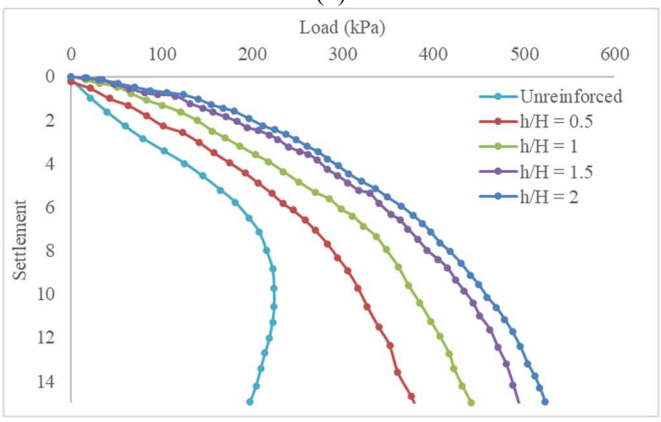


(c)

Fig. 7. Load-settlement ratios for different height of the geocell for different relative densities (a) 30% (b) 50% and (c) 70%

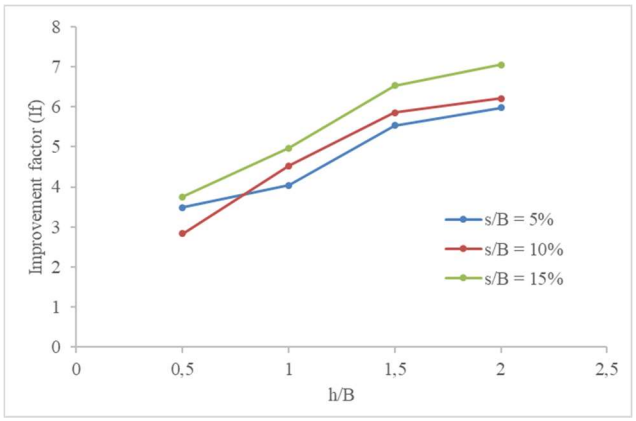


(a)

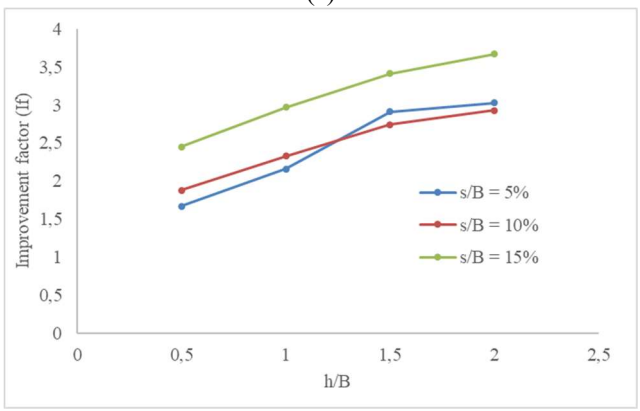


(b)

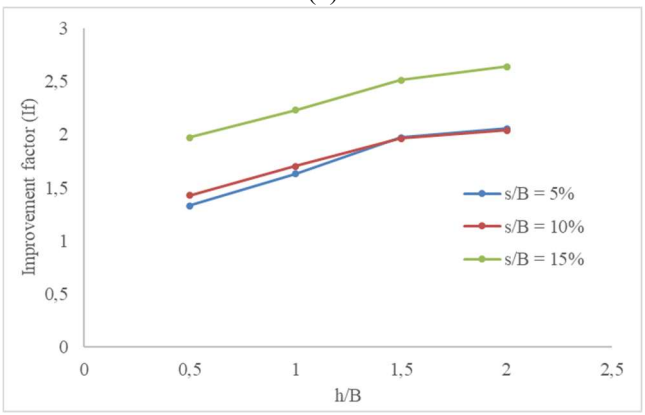


(c)

Fig. 8. Variation of improvement factor ($I_f$) for different height (h) of the geocell at different relative densities (a) 30% (b)50% and (c)70%

Table 4. Summary of improvement factor ($I_f$) at different settlement ratios for tests S. No. (2-4)

| S. No. | Variable parameters | Improvement factor ($I_f$) | | |
|---|---|---|---|---|
| | | s/B = 5% | s/B = 10% | s/B = 15% |
| 2 | u = 0B | 3.25 | 3.63 | 4.13 |
| | u = 0.1B | 5.01 | 5.25 | 6 |
| | u = 0.2B | 4.54 | 4.96 | 5.2 |
| | u = 0.3B | 4.57 | 4.72 | 4.98 |
| | u = 0.4B | 4.37 | 4.48 | 4.78 |
| 3 | b = 1B | 3.65 | 3.74 | 3.9 |
| | b = 2B | 4.06 | 4.84 | 5.42 |
| | b = 3B | 4.89 | 5.26 | 5.94 |
| | b = 4B | 5.43 | 5.97 | 6.53 |
| | b = 5B | 5.85 | 6.2 | 6.76 |
| 4 | h = 0.5B, $R_d$ = 30% | 3.49 | 2.83 | 3.75 |
| | h = 1B, $R_d$ = 30% | 4.04 | 4.53 | 4.97 |
| | h = 1.5B, $R_d$ = 30% | 5.53 | 5.85 | 6.53 |
| | h = 2B, $R_d$ = 30% | 5.97 | 6.21 | 7.05 |
| | h = 0.5B, $R_d$ = 50% | 1.66 | 1.88 | 2.45 |
| | h = 1B, $R_d$ = 50% | 2.16 | 2.33 | 2.97 |
| | h = 1.5B, $R_d$ = 50% | 2.91 | 2.74 | 3.41 |
| | h = 2B, $R_d$ = 50% | 3.03 | 2.93 | 3.67 |
| | h = 0.5B, $R_d$ = 70% | 1.33 | 1.42 | 1.97 |
| | h = 1B, $R_d$ = 70% | 1.63 | 1.7 | 2.23 |
| | h = 1.5B, $R_d$ = 70% | 1.97 | 1.96 | 2.51 |
| | h = 2B, $R_d$ = 70% | 2.05 | 2.04 | 2.64 |

## 4.4. Effect of relative density of sand

To analyse the effect of sand relative density ($R_d$) on the behaviour of a geocell reinforced foundation system, three different relative densities ($R_d$) of 30%, 50%, and 70% were used in the numerical analysis. Improvement factor ($I_f$) obtained for different relative densities ($R_d$) are presented in Table 5 (S. No. 4). The results

show that the improvement factor decreases as the relative density of sand increases. The improvement factor at settlement ratio 15% and h/B ratio 2 for relative density 30% is 7.05 and for relative densities 50% and 70%, the improvement factor was reduced to 3.67 and 2.64. The load settlement plots shown in Fig. 8, shows that for relative density 30% and 50% the unreinforced soil foundation system have shown local shear failure and for 70% relative density general shear failure has been observed. In loose sand, there is a greater number of voids are available, therefore soil gets contract on the application of the load and more strain is required to transfer the stress on the walls of the geocell, although for the soil having high relative density, being a rigid structure leads to expand on the application of footing load and all the strain is transferred on the walls of the geocell. Hence, results in higher improvement factor obtained in loose sand compared to dense sand.

## 4.5. Displacement contours

The vertical displacement contours for square footings lying on unreinforced and geocell reinforced sand are shown in Figure 9. Contours are presented at a settlement ratio (s/B) of 15%. The present contours of the displacement are depicted its significance to analyse the actual displacement under the given load. From the analysis of the displacement contours depicted that the maximum displacement was perceived in case of unreinforced sand whereas in case of geocell reinforced sand at least 5 – 6 times higher load is required compared to unreinforced sand. Furthermore, from the analysis of these figures indicate that the displacement contours of unreinforced and geocell reinforced foundation bed remains firmly established within the designated lateral and vertical boundaries. This indicate that the chosen boundaries in horizontal and vertical direction are sufficient for the given problem.

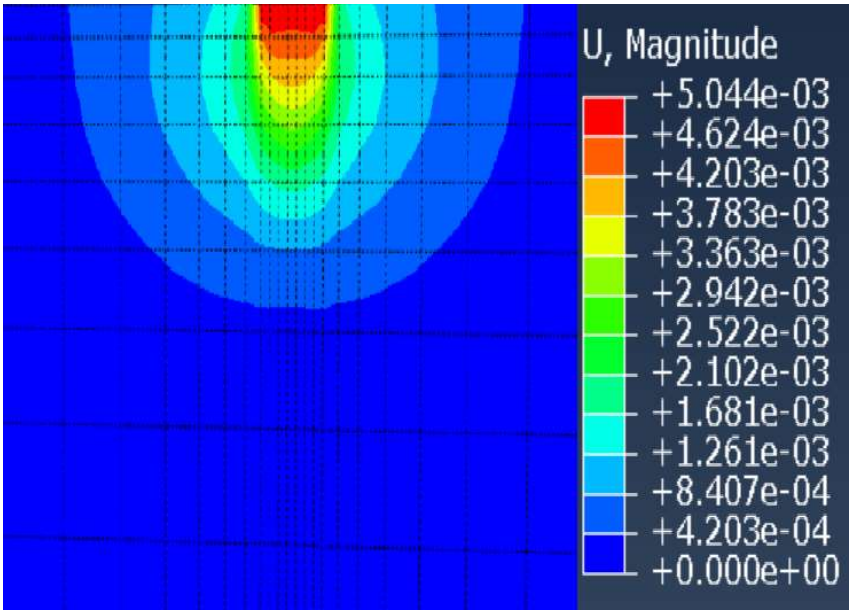


(a)

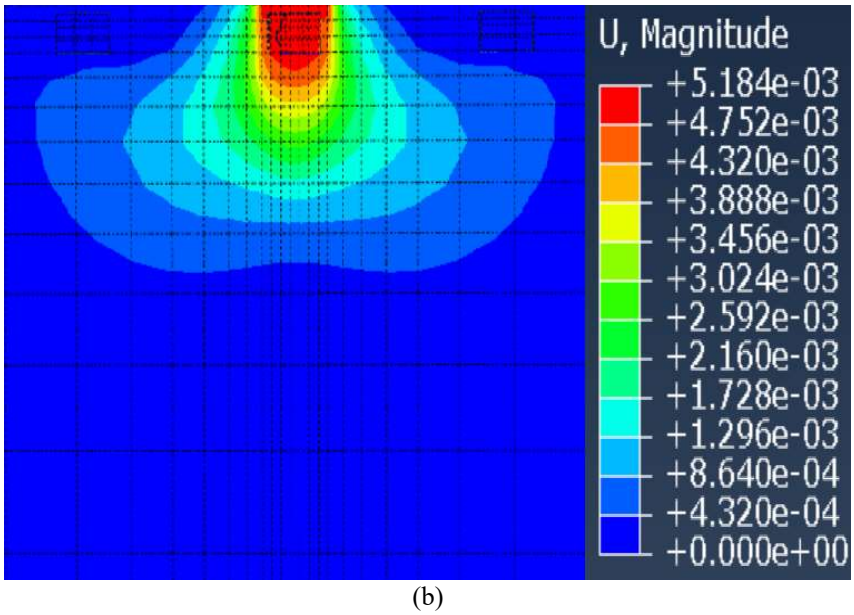


(b)

Fig. 9. Displacement contours for (a) unreinforced sand and (b) geocell reinforced sand

### 4.6. Comarision with literature

The numerical modelling results of the present study were compared with the experimental results of square footing rested on geocell reinforced sand presented in literature [10]. The square footing of size 150mm and tank dimension 750mm × 750mm × 750mm were used in the experimental work. The peak friction angle and cohesion value calculated from triaxial compression test were reported as 38˚ and 0 respectively. In the experimental investigation, the minimum and maximum unit weights of sand were reported as 13.8 and 15.9 kN/m3, respectively. To compare the numerical modelling findings, the unit weight and friction angle of the sand were taken 16.2 kN/m3 and 39.08, respectively, corresponding to a relative density of 50%. The geocell depth was varied as 0.5B, 1B, 1.5B and 2B with constant wall thickness of the geocell 1.5mm similarly presented in study [10]. The comparison of numerical modelling findings with experimental data as shown in Table 5. The comparative findings show that the average variation in bearing capacity was determined to be 7.35 percent, which was due to the higher value of the mass density and friction angle of the sand was taken in the numerical analysis.

Table 5. Comparison of numerical modelling results with literature

| Bearing capacity ($q_u$) at prescribed displacement ratio (s/B) of 15% | | |
|---|---|---|
| h/B | [10] | Present study |
| 0 | 137.14 | 144.16 |
| 0.5 | 301.14 | 339.96 |
| 1 | 393.80 | 420.22 |
| 1.5 | 461.79 | 483.58 |
| 2 | 429.69 | 520.37 |

## 5. CONCLUSION

A numerical analysis was performed in this paper to evaluate the effect of geocell reinforcement on the load settlement behaviour of square footings placed on sand using variable geometric parameters of the geocell. This study has also analyse the effect of relative density of sand on the performance of the geocell reinforcement. The following conclusions can be drawn from the results presented above:

1. The provision of the geocell reinforcement in sand enhances the load settlement behaviour of the shallow footing by 5 – 6 times compared to unreinforced sand.
2. The optimum depth of the geocell reinforcement below the footing base was observed at 0.1B. Furthur increasing the placement depth of the geocell layer tends to decrease the performance of the geocell due to lateral mobilization of sand on the application of footing load.
3. A significant improvement in load carrying capacity was observed at a width four times the footing size, beyond this width very little improvement was noted..
4. The maximum benefit of the geocell reinforcement is obtained at a height of geocell equal to 1.5B, beyond this height the improvement get reduced due to buckling of the geocell walls on the increment of load.
5. Geocell reinforcement has been proven to be more benificial in the case of loose sand compared to dense sand. The improvement factor obtained for 30% relative density at optimum combination of the geocell geometry i.e u = 0.1B, b = 4B and h = 1.5B is 6.53 and for 50% and 70% relative density improvement factor was reduced to 3.41 and 2.51.

The present study results were purely based on FEM based numerical study conducted on square footing placed on geocell reinforced sand using variable geometric combination of geocell reinforcement. However, experimental study is recommended to validate the numerical analysis results presented in this study by using same footing dimension and geometric parameters of the geocell. The proposed numerical study could be helpful for the civil engineers to design the optimum combination of the geocell reinforcement for the sand below the footing base.

## NOTATION

u = Depth of geocell below the footing base
b = Width of geocell
h = Height of geocell
B = Width of footing
s/B = Settlement ratio
t = Thickness of gocell wall
$\gamma$ = Unit weight
E = Modulus of elasticity
$\mu$ = Poisson's ratio
$R_d$ = Relative density
Ø = Friction angle
$\Psi$ = Dilation Angle

c = Cohession
δ = Interface friction Factor

## ACKNOWLEDGEMENT

I would like to express my special thanks of gratitude to Central Building Research Institute (CSIR-CBRI) Roorkee for providing me the opportunity to utilize the ABAQUS software.

## REFERENCES

1. Nazir, AK and Azzam, WR 2010. Improving the bearing capacity of footing on soft clay with sand pile with/without skirts. *Alexandria Engineering Journal* **4**, 371–377. DOI: https://doi.org/10.1016/j.aej.2010.06.002
2. El Wakil, AZ 2010. Horizontal capacity of skirted circular shallow footings on sand. *Alexandria Engineering Journal* **49**, 379–385. DOI: https://doi.org/10.1016/j.aej.2010.07.003
3. Khatri, VN et al. 2019. Numerical study on the uplift capacity of under-reamed piles in clay with linearly increasing cohession. *International journal of geotechnical engineering* 1-12.
4. Sitharam, TG et al. 2005. Model studies of a circular footing supported on geocell-reinforced clay. *Canadian Geotechnical Journal* **42**, 693–703. DOI: https://doi.org/10.1139/t04-117
5. Shukla, SK 2012. *Handbook of geosynthetic engineering*, Landon: ICE Publications.
6. Dash, SK et al. 2003. Model studies on circular footing supported on geocell reinforced sand underlain by soft clay. *Geotextiles and Geomembranes* **21**, 197–219. DOI: https://doi.org/10.1016/S0266-1144(03)00017-7.
7. Dash, SK et al. 2007. Behaviour of geocell-reinforced sand beds under strip loading. *Canadian Geotechnical Journal* **44**, 905–916. DOI: https://doi.org/10.1139/T07-035
8. Sireesh, S et al. 2009. Bearing capacity of circular footing on geocell-sand mattress overlying clay bed with void. *Geotextiles and Geomembranes* **27**, 89–98. DOI: https://doi.org/10.1016/j.geotexmem.2008.09.005.
9. Hegde, A and Sitharam, TG 2017. Joint Strength and Wall Deformation Characteristics of a Single-Cell Geocell Subjected to Uniaxial Compression. *International Journal of Geomechanics* **15**. DOI: https://doi.org/10.1061/(asce)gm.1943-5622.0000433
10. Sherin, KS et al. 2017. Effect of Geocell Geometry and Multi-layer System on the Performance of Geocell Reinforced Sand Under a Square Footing.

*International Journal of Geosynthetics and Ground Engineering* **3**, 1-11. DOI: https://doi.org/10.1007/s40891-017-0097-3

11. Dehkordi, PF et al. 2021. Bearing capacity-relative density behavior of circular footings resting on geocell-reinforced sand. *European Journal of Environmental and Civil Engineering* 1-25. DOI: https://doi.org/10.1080/19648189.2021.1884901
12. Muthukumar, S et al. 2019. Performance Assessment of Square Footing on Jute Geocell-Reinforced Sand, *International Journal of Geosynthetics and Ground Engineering* **5**, 1-10. DOI: https://doi.org/10.1007/s40891-019-0176-8
13. Latha, GM and Murthy, VS 2007. Effects of reinforcement form on the behavior of geosynthetic reinforced sand. *Geotextiles and Geomembranes* **25**, 23–32. DOI: https://doi.org/10.1016/j.geotexmem.2006.09.002
14. Hegde, A and Sitharam, TG 2013. Experimental and numerical studies on footings supported on geocell reinforced sand and clay beds. *International Journal of Geotechnical Engineering* **7**, 346–354. DOI: https://doi.org/10.1179/1938636213Z.00000000043
15. Mehdipour, I et al. 2013. Numerical study on stability analysis of geocell reinforced slopes by considering the bending effect. *Geotextiles and Geomembranes* **37**, 23–34.
    DOI: https://doi.org/10.1016/j.geotexmem.2013.01.001
16. Yang, X et al. 2012. Accelerated pavement testing of unpaved roads with geocell-reinforced sand bases. *Geotextiles and Geomembranes* **32**, 95–103. DOI: https://doi.org/10.1016/j.geotexmem.2011.10.004
17. Yünkül, K et al. 2021. Numerical Analysis of Geocell Reinforced Square Shallow Horizontal Plate Anchor. *Geotechnical and Geological Engineering* **39**, 3081-3099. DOI: https://doi.org/10.1007/s10706-021-01679-1
18. Dehkordi, PF et al. 2019. Effect of geocell-reinforced sand base on bearing capacity of twin circular footings. *Geosynthetics International* **26**, 224-236. DOI: https://doi.org/10.1680/jgein.19.00047
19. Astaraki, F et al. 2022. Effect of Geocell, on the Mechanical Behavior of Railway Embankments, Using FE Modeling. *Acta Polytechnica Hungarica*, *19*(6).
20. Jayanthi, V. et al. 2022. Influencing Parameters on experimental and theoretical analysis of geocell reinforced soil. *Materials Today: Proceedings*.
21. Anusha Raj, K et al. 2022. Critical Overview of Reinforcing Sand Using Geocell for Shallow Foundation. *Advances in Construction Materials and Sustainable Environment*, 271-280.
22. Sharma, M, Inti, S, Tirado, C and Tandon, V 2016, Evaluating the benefits of geocell reinforcement of the base course in flexible pavement structures using

3-d finite element modeling. *International Conference on Transportation and Development*.
23. Biabani, MM et al. 2016. Modelling of geocell-reinforced subballast subjected to cyclic loading. *Geotextiles and Geomembranes* **44**, 489–503. DOI: https://doi.org/10.1016/j.geotexmem.2016.02.001
24. Fattah, MY et al. 2018. Behavior of flexible buried pipes under geocell reinforced subbase subjected to repeated loading. *International Journal of Geotechnical Earthquake Engineering* **9**, 22–41. DOI: https://doi.org/10.4018/IJGEE.2018010102
25. Satyal, SR et al. 2018. Use of cellular confinement for improved railway performance on soft subgradese. *Geotextiles and Geomembranes* **46**, 190–205. DOI: https://doi.org/10.1016/j.geotexmem.2017.11.006
26. Ari, A and Misir, G 2021. Three-dimensional numerical analysis of geocell reinforced shell foundations. *Geotextiles and Geomembranes* **49**, 963–975. DOI: https://doi.org/10.1016/j.geotexmem.2021.01.006
27. Zhang, L et al. 2010. Bearing capacity of geocell reinforcement in embankment engineering. *Geotextiles and Geomembranes* **28**, 475–482. DOI: https://doi.org/10.1016/j.geotexmem.2009.12.011
28. Neto, JOA 2019. Application of the two-layer system theory to calculate the settlements and vertical stress propagation in soil reinforcement with geocell. *Geotextiles and Geomembranes* **47**, 32–41. DOI: https://doi.org/10.1016/j.geotexmem.2018.09.003
29. Acharyya, R and Dey, A 2017. Finite Element Investigation of the Bearing Capacity of Square Footings Resting on Sloping Ground. *INAE Letters* **2**, 97–105. DOI: https://doi.org/10.1007/s41403-017-0028-6
30. Hegde, A and Sitharam TG 2008. 3-Dimensional numerical modelling of geocell reinforced sand beds. *Geotextiles and Geomembrane* **43**, 171-181. DOI: http://dx.doi.org/10.1016/j.geotexmem
31. Bolton, MD 1986. The strength and dilatancy of sands. *Geotechnique* **36**, 65–78. DOI: https://doi.org/10.1680/geot.1986.36.1.65
32. Bowles JE 1977. Foundation analysis and design. New York: McGraw- Hill.
33. Kulhawy, FH and Mayne, PW 1990. Manual on estimating soil properties for foundation design. United States: Geotechnical Engineering Group.

*Editor received the manuscript: 01.04.2022*